Continuous, high-throughput flash-synthesis of submicron food emulsions using a confined impinging jet mixer

Siddiqui, Shad W.; Wan Mohamad, W. A. F.; Mohd Rozi, M. F.; Norton, Ian T.

DOI:
10.1021/acs.iecr.7b02124

Continuous, High-Throughput, Flash-Synthesis of Submicron Food Emulsions Using a Confined Impinging Jet Mixer: Effect of *In Situ* Turbulence, Sonication and Small Surfactants

Shad W. Siddiqui[1], W.A.F. Wan Mohamad, M.F. Mohd Rozi and Ian T. Norton

School of Chemical Engineering, University of Birmingham, Birmingham B15 2TT, UK.

[1] Shad.Siddiqui@innotechalberta.ca (corresponding author)

Shad W. Siddiqui: InnoTech ALBERTA (Formerly, Alberta Innovates - Technology Futures), 250 Karl Clark Road, Edmonton, Alberta T6N 1E4, Canada (Present address)
W.A.F. Wan Mohammad: Centre of Biospectroscopy, School of Chemistry, Monash University, Clayton, Victoria 3800, Australia (Present address)
M.F. Mohd. Rozi: Brooke Dockyard and Engineering Works Corporation, Kg. Sejingkat, Jalan Bako, 93050 Sarawak, Malaysia (Present address)

ABSTRACT

Reproducible quality of emulsions with high throughput is critical for a variety of specialized applications such as pharmaceutics and foods. In this work we propose a simple and effective approach for producing highly stable, submicron size oil-in-water emulsions by high-shear, controlled turbulence in confined impinging jet mixer using commercial-grade components and low molecular weight emulsifiers. Targeting the submicron range, food-grade oil-in-water emulsions in the 100 nm to 1 μm size range have been produced by synergistically coupling multi-pass, jet-induced turbulence and ultrasonication effects to produce a throughput of up to 1.2 L/min. The mixer was easy to fabricate and operate. In addition, physiochemical effects of small molecule emulsifiers or surfactants and their formulations on drop breakup and stability were found to be important and were investigated to determine the optimal emulsifier deployment strategy. Other determining variables like magnitude and duration of local turbulence/energy dissipation and relative effects of competing process timescales were considered to explain the obtained results. Furthermore, several mixhead schemes were designed and tested to enhance local turbulence within the mixing volume. There is ample evidence that the confined turbulent impinging jet mixer can therefore accelerate the development of specialized emulsion-based products/applications by providing a robust platform for synthesis of submicron and nano emulsions with precise properties at industrially relevant scales.

KEYWORDS submicron emulsions, turbulence, confined impinging jet mixer, drop breakup, drop coalescence, interfacial tension and process timescales

1. INTRODUCTION

Submicron systems are defined as fine emulsion dispersions with drop sizes in the submicron or nano range. Over the past decade or so they have gained popularity due to a number of unique functional characteristics such as high surface area, robust stability, tunable rheology and appealing appearance. Due to the size characteristics, submicron emulsions achieve high stability against creaming and coalescence, which makes them an excellent carrier system for a wide variety of active ingredients.

The quality and stability of emulsions play a major role in refining the physical characteristics and effectiveness of numerous end products. Submicron emulsions have gained a lot of attention in the development of colloidal drugs and as carrier systems for actives in functional foods, pharmaceuticals, cosmetics and personal care products[1-3]. Depending on the application, submicron drops could improve solubility, texture, aesthetics, mouthfeel, rheology, shelf-life, or even cost. Leveraging the high surface area, they have also shown higher capacity to encapsulate actives and in controlled-release of the incorporated micronutrients[4].

In pharmaceutical applications emulsions are one of the most commonly used drug vehicles for poorly water-soluble drugs due to the unique advantage in mass manufacturing and easy sterilization[5]. Submicron injectable emulsions have been gaining attention as a vehicle for the intravenous administration of lipophilic drugs[1]. Few drugs have been successfully formulated as submicron emulsions and some novel emulsion formulations have exhibited improved pharmacological activity, underlying the promising therapeutic properties of colloidal vehicles for potent lipophilic drugs[1]. The physicochemical stability of submicron emulsions

incorporated with a mixture of drugs is the main factor limiting a wider use of this vehicle for administration[2]. In few cases, excellent physiochemical stability has also been observed[5].

Emulsification process is a two-step dynamic process that involves drop breakup and re-coalescence which together determine final drop size of the disperse phase[6]. If not fully stabilized, newly formed drops being thermodynamically unstable are susceptible to coalescence. This is also favored by the Brownian motion of the drops, which effectively leads to collisions and subsequent coalescence[7]. Drop coalescence, during collision, is often the limiting factor in drop size reduction process[8].

Emulsion preparation methods are often directed by intended end user-specific applications. Current techniques of emulsification include batch-type contactors which tend to have limited reproducibility and control over physicochemical characteristics of the synthesized emulsion product. Contrary to this, continuous synthesis techniques may provide precise control of the process variables and better control over product characteristics, overall quality, and reproducibility, which is especially relevant for specific applications such as pharmaceutics and food. Thus, a broader classification can be made based on energy requirements of the synthesis methods, such as low-energy or energy-intensive methods. The most widely used preparation methods for submicron/nano emulsions include high energy methods though low energy methods may be used depending on industrial relevancy. However, there is often little understanding of industrial relevance of many of these preparation approaches as rational scale-up rules have not been widely explored. Based on the desired end-product characteristics, submicron or nano emulsions may be desired. Often a low polydispersed and smaller drop size system may be required for pharmaceutical and drug delivery applications than for food and generic cosmetic applications.

Low-energy methods include phase inversion[9] or membrane emulsification and are less favored due to limited capacity for producing emulsions at large scale for industrial use and the high surfactant concentration requirement[10, 11]. In contrast, high-energy methods are more common and relevant industrially due to flexible control of drop size distribution and the ability to produce fine emulsion drops. Such techniques include rotor-stator, high-pressure homogenizers, microfluidizers, jet dispersers, and ultrasonic equipments.

High-pressure homogenizers (HPH) are commercially used in the food industry to produce dairy emulsions[12], where most of the drop break up occurs around the valve edges[13]. Fine drops are, however, achievable only at a very high pressure of up to 700 MPa[14]. By virtue of a simpler design, homogenizers may be easy to scaleup but tight control on emulsion quality may be difficult to maintain. Typical size variation (polydispersity) in a HPH is an order of magnitude different at operating pressure of 15,000 psi[15, 16]. By contrast, microfluidizers may be better equipped to produce smaller-size emulsions at similar operating pressures by virtue of its geometric design[15]. Typical microfluidizer design consists of a small chamber where two inlet jets of around 100-150 μm diameter collide at 180° and most of the drop breakup occurs at the impingement region in outer regions of the jets. The jets are pressurized to create relevant shear for drop break-up. Though widely used within the highly specialized pharmaceutical industry; the production rate of a microfluidizer is however low and as such they may not be suitable for relevantly large production rates as for the low cost food and beverage industry. Labscale microfluidizers typically produce a flow rate of 120 mL/min at an operating pressure of 30,000 psi while a full scale industrial scale models produce a flow of 2-4 L/min at a pressure of 40,000 psi[17]. Microfluidizer processing produces a Gaussian drop

size distribution where drop size polydispersity is an order of magnitude different between the produced drop sizes i.e. smallest to the largest drops[15].

Recently, the ability of impinging jet configurations to synthesise consumable macro emulsions (<4 μm), on a continuous basis, has been harnessed to enhance the controllability and reproducibility of emulsions[18]. Co-linear impinging jets (CIJ) have been designed such that the inlet feed passing through 1000 μm (1 mm) diameter tubes is forced through a narrow mixing zone experiencing high turbulence just above the atmospheric pressure (~15 psi). Peak mixing region is typically ~3.1×10^{-5} mL in size and continuous feed injection ensures that the feed streams experience highest shear condition and rapid drop size reduction at any given jet flow rate. Another advantage of high speed injection is the small residence time that reduces drop-drop collisions and allowing for a relatively narrower PSD. The drop sizes are known to exhibit dependence on the duration of shear treatment[13] and may scaleup with the mixer residence time.

The intended approach to produce submicron emulsions is to enhance formation of smaller drops by controlling surfactant-assisted coalescence as well as shear-assisted drop breakup. On the surfactant/emulsifier side we study how small surfactants and their formulations could aid in small drop deformation, drop break up and drop stabilization. On shear side, we examine how mixhead geometry can be modified to enhance local turbulence and the energy dissipation at the microscale (Kolmogorov lengthscale).

In the following sections, we demonstrate and characterize various configurations of a labscale confined impinging jet mixer (CIJ), simple in design and fabrication, in combination with aggressive ultrasonic cavitation to produce submicron emulsions, through a top-down

approach. The modified CIJ can produce 1.2 L/min of product flow at industrially relevant-scales, while retaining the advantages of homogeneity, reproducibility and tunable control over emulsion characteristics at operating atmospheric pressure (~15 psi) condition. CIJ can be constructed in different schemes but in co-linear, head-on impinging jets scheme with one outlet (Figure 1b) is most common[13, 18]. Another variation is a scheme with two outlets (Figure 1a) which can reduce the back pressure arising from co-axial jets impingement and reduce possible collisions between newly created drops.

Our aim is to propose a mechanism for producing submicron emulsion drops, and to define a strategy to keep the drops stabilized in that size range. This has been achieved by systematically studying process hydrodynamics in various CIJ schemes where secondary turbulence is provided through a sonotrode that creates acoustic cavitation and flash stabilizing the produced drops. Whereas about 3.9% to 5.4% of the electrical energy is converted to mechanical vibrations over a tiny fluid volume during ultrasonication[19, 20]; some studies report higher efficiencies of 50% to 90%[21, 22]. The success of synergetic approach will depend on good macromixing in the primary impingement region, which essentially brings a continuous supply of the emulsion to the vibrating face of the probe.

We thereon demonstrate the versatility of the turbulent CIJ mixer by combining jet hydrodynamics and sonication mechanisms to enhance local turbulence and drop breakup. Higher turbulence may overcome any turbulence dampening arising due to higher oil content, and may be able to produce fine emulsions with consistent drop size distribution. The designed submicron emulsions will be characterized and we hope is that our results will generalize the desired characteristics of submicron emulsions for various practical applications.

2. MATERIAL AND METHODS

2.1 Materials

The disperse phase, sunflower oil (Solesta , UK), was procured locally and used without further modifications, while the continuous phase, double-distilled water (conductivity ~ 1.4 μS/cm, pH = 6.8), was available in the laboratory. Three surfactants with specific concentrations (higher than the critical micelle limit) were used to emulsify the sunflower oil and to stabilize the oil drops. The surfactants with different HLBs were Tween 20 (polyoxyethelene-20-sorbitan monolaurate, CAS: 9005-64-5; Sigma-Aldrich UK) at 1 wt%, SDS (sodium dodecylsulphate, CAS: 151-21-3; Fisher Scientific UK) at 0.5 wt%, and PGPR (polyglycerol polyricinoleate or E476 or Plasgaard 4150, CAS: 29894-35-7; Palsgaard) at 0.5 wt%. While the first two surfactants were solubilized in the continuous phase (water), PGPR of opposing HLB was dissolved in the disperse phase (oil) prior to forming pre-emulsion to examine the effects of single and/or surfactant formulation on the disperse drop size and drop size distribution. Later, silicone oil (polydimethylsiloxane, CAS: 63148-62-9; Aldrich Chemistry) with equivalent viscosity of 50 cP was used in some experimental runs. The commercial grade sunflower oil may have contained some dissolved biosurfactants but any change in interfacial tension due to them was discounted in this work.

2.2 Experimental

Oil-in-water pre-emulsions were prepared by homogenizing 5% (v/v) and 10% (v/v) sunflower oil in 1 wt% Tween20 and 0.5 wt% SDS solutions at an impeller speed of 2,000 rpm for 10 minutes using a Silverson SL2T mixer under room conditions. A low volume percentage of the oil phase was chosen to minimize collision between the drops. Further to

this, PGPR co-emulsifier was introduced to the oil phase at 0.5 wt% prior to mixing the oil phase with the aqueous surfactant solution. The pre-mixing procedure helped to reduce the difference in the size distribution by keeping the volume fraction of drops and feed stream viscosities relatively constant[23].

The emulsion was further refined by pumping the pre-emulsion through confined impinging jet mixhead (CIJ). Two schemes of CIJ, shown in Figure 1a (mixhead MH-1) and Figure 1b (Mixhead MH-2), were tested. Figure 1 (b) is a well-characterized geometry, which has been studied extensively[13, 18, 24, 25], while modified mixhead MH-1 is designed with two outlets. The minimal rise in temperature (0.1˚C) due to any viscous dissipation was measured but did not have any marked effect on the fluid properties. The original mixhead design (MH-2) was later modified to accommodate a sonic probe within the mixhead, such that the flat tip of the probe (3.18 mm diameter) replaced the hemispherical portion of the mixhead. Figure 1c presents the modified mixhead. The secondary energy input for emulsification was provided through the sonication probe containing a piezoelectric quartz crystal that expanded and contracted in response to the alternating electrical voltage. The ultrasonic effect produced cavitation due to mechanical vibrations at the contact area of the probe with the liquid. The sonicator (VCX 500, SONICS) was operated at a frequency of 20 kHz and a maximum output power of 500 W. The input energy was varied from 0 W (0% amplitude) to 200 W (40% amplitude) with sonication efficiency varying between 3.9%[19] and 50%[21, 25], estimated from calorimetric measurements. A temperature increase at this juncture would have helped to reduce viscosity of the dispersed phase and enhance interfacial kinetics. For higher flow visibility, the mixheads were fabricated out of Perspex fibreglass.

Pulseless gear pumps (Series GB, IDEX Corporation, max flow rate 4 L/min) were used to feed pre-emulsion to the mixheads. The inlet feed rates were varied from 44 mL/min (Re_{jet} = 1000, $Re_{jet} = d_{jet}.V_{jet}.\rho_c/\mu_c$) to 843 mL/min ($Re_{jet}$ = 18,000) to study the effect of colliding streams. The pumps were calibrated by mass and volumetric methods for the entire range of flow rates investigated. Dye experiments were conducted to establish the physical stability of the colliding jets and to establish optimum operational flowrate limits for high energy density (turbulent energy dissipation, ε) within the mixhead.

All emulsions samples produced from CIJ were characterized in size and range by dynamic light scattering (DLS) method using Mastersizer 2000 (Malvern Instruments, UK). Each sample was first diluted with double-distilled water to 1% (v/v) concentration to avoid multiple scattering effects in concentrated samples. Samples were measured after a few minutes of alignment at room temperature and d_{32} results were recorded as the average of three measurements. At least three sample repeats were done to establish the standard deviation (< 10%) over the experimental range. The drops were imaged with an optical microscope (POLYVAR) for comparison to the DLS data from the Mastersizer 2000. All interfacial tension measurements were conducted on a Wilhelmy plate (Kruss Germany).

3. RESULTS AND DISCUSSION

The experimental results are presented in five sections with each considering the effect of a single operating variable on mean drop size (d_{32}) and the size distribution. In Section 3.1, the effect of jet flow rate on drop size through mixhead MH-1 is studied. Several surfactants were used either singly or in combination with a co-emulsifier/co-surfactant. A comparison

between mixhead schemes MH-1 and MH-2 was also made using the same surfactant formulations. Similarly, in Section 3.2, mixhead geometries MH-1 and MH-2 are compared in terms of the obtained drop sizes under recirculation conditions. In Section 3.3, drop data for mixhead MH-2, integrated with an ultrasonic probe, is presented. In Section 3.4, physical stability of the produced emulsions was also recorded over a period of several weeks and is discussed. In Section 3.5, process timescales of the competing mechanisms are discussed to support the experimental data. Finally, in Section 3.6, emulsification performance of CIJ is compared with the prevalent nano-emulsification techniques.

3.1 Effect of jet flow rate and geometric design

Three types of surfactants and four formulations were selected for emulsion preparation. Those used were: (a) 1 wt% Tween20, (b) 1 wt% Tween 20 with 0.5 wt% PGPR, (c) 0.5 wt% SDS, and (d) 0.5 wt% SDS with 0.5 wt% PGPR. Different surfactants were distinguished based on their interfacial tensions (o/w) and molecular sizes. Comparing SDS and Tween20, SDS reached a lower o/w interfacial tension (0.78±0.17 mN/m) than Tween20 (6.06±0.03 mN/m) with the dispersed sunflower oil in water continuous phase.

Suitable mixheads MH-1 and MH-2 were also designed and tested. Mixhead MH-1 was conceptualized to reduce the back pressure within MH-2 scheme and to enhance local turbulence. High turbulence would help in the formation of smaller drops and would narrow down the drop size distribution. To verify this, experiments with emulsifier combinations including SDS only, SDS with PGPR, Tween20 only, and Tween20 with PGPR were carried out in the modified mixhead MH-1. Consequently, the best formulation delivering the

smallest drop sizes was identified and re-tested with mixhead MH-2 to compare the emulsification performance of the two mixhead schemes.

Figure 2 (a) presents emulsion size data obtained for mixhead MH-1 at single pass at varying inlet jet flow rates. Data shows that smaller emulsion drops were a direct result of an increase in jet flow rate and hence the Re_{jet} number. This was true for all emulsified systems, particularly beyond 105 mL/min ($Re_{jet} \approx 2{,}200$). However, below this value there were fluctuations in drop size data, which were due to a transitional flow regime that was unstable. This was also evident by the lower data repeatability at smaller jet flow rates. Tween20 emulsified system depicted a more significant drop in the drop size with flow rate compared to SDS. This may be related to the difference in molecular structure between Tween20 and SDS. The Tween20 molecule has a larger head group[26] of 0.97 nm^2 and a branched molecule with a molecular weight of 1,228 g/mol. It may have diffused relatively slowly to the interface compared to an SDS molecule with a head size[27] of 0.55 nm^2 and a linear molecule with a smaller molecular weight of 288. Both systems however showed a similar gradual drop in drop size as full turbulence was approached. Adsorption timescales for the two emulsifiers at the o/w interface were expected to be similar because the convective transfer from the bulk to the interface was rate limiting which reduced significantly under turbulent flow conditions. Drop data for formulations (SDS-with-PGPR and Tween20-with-PGPR) was slightly smaller than the drop sizes obtained with single emulsifiers, indicating that combined emulsifiers were performing slightly better than the single emulsifiers. With surfactants present on both sides of the interface (oil-soluble and water-soluble), interfacial stabilization is expectedly quicker. Further, Figure 2(b) presents the drop size distribution of Tween20 emulsified system. It is obvious, that the peak representing the mode of the distribution shifted to the left

as the jet flow rate was increased from 55 mL/min ($Re_{jet} \approx 1,200$) to 843 mL/min ($Re_{jet} \approx 17,900$). Considering the area under the curve, the number of drops with a size smaller than that of the mode rose considerably with feed flow rate, indicating that more drops were being sheared and broken into smaller ones. This was further confirmed by the micrographs in inset in Figure 2, obtained from the three samples that were used to determine the above drop size distributions. The lowest flowrate resulted in a wider drop size distribution which is likely due to the uneven drop break up in the transitional flow regime within the mixer at low Reynolds number. Few smaller droplets that likely formed as a result of drop elongation and pinch-off mechanism appear to surround and sit above the largest drops. This may have happened during sample preparation for light microscopy. The polydispersity, in general, appears to reduce at higher flowrates, as the flow becomes fully turbulent.

Next, Table 1 presents minimum mean drop sizes obtained after multiple passes for each of the emulsified systems, under full turbulence (843 mL/min, $Re_{jet} = 17,900$) in MH-1 mixhead. Comparing Tween20 and SDS, the latter seems to be a better emulsifier for the sunflower oil-in-water system, having delivered smaller drops than Tween20. This may again be explained by the relatively small head size and tail length of the SDS molecule relative to that of Tween20, which can adsorb faster on the oil interface, thus giving a higher packing density and drop stabilization. It was also observed that surfactant formulation yielded better results than did the single surfactants or emulsifiers. The performance of combined surfactants was better, perhaps due to closer packing of the surfactant molecules on the drop interface.

Furthermore, emulsification performances of mixhead schemes MH-1 and MH-2 are compared in the presence of Tween20-PGPR formulation. Both these emulsifiers are of great interest to us as they find extensive use in food applications. These results are presented in

Figure 3. The SDS-PGPR formulation is left out of the comparison due to the limited number of food and potential pharmaceutical applications.

Figure 3 presents drop size data for mixheads MH-1 and MH-2 for Tween20-PGPR formulation. Drop size data shows that the performance of two geometries are comparable in terms of the reducing drop sizes with increasing flow rates, reaching a minimum drop size (~5 μm) beyond a certain flow rate and Reynold number. This is because the graphs converge at the feed flow rate of 410 mL/min ($Re_{jet} \approx 10{,}000$) and little effect was observed beyond the onset of full turbulence by increasing the flow rate. The emulsification performance of mixheads MH-1 and MH-2 are therefore comparable in terms of the drop sizes obtained under equivalent turbulence. Drop sizes could, therefore, be controlled reproducibly by tuning Re_{jet}. In addition, the effect of small differences in relative viscosities and densities between the two streams is negligible under fully a turbulent flow condition, which makes both the schemes very robust in operation.

The energy available for mixing (emulsification) is estimated by doing a macroscopic mechanical energy balance over the CIJ mixhead, considering the potential energy, kinetic energy and pressure energy[25]. In a flow system, the sum of the changes in each of the energy components together determines the energy dissipated due to friction and shear. This loss in energy is the energy dissipated at the smallest length-scales (Kolmogorov scale) in the fluid. A mechanical energy balance is therefore applied over the inlet and the exit planes in CIJ mixer to determine the rate of energy dissipation (ε) within the mixing control volume. Total energy contribution for energy dissipation came from the pressure drop and changes in fluid kinetic energy from the inlets (nos. 1 and 2) to the exit (nos. 3) of the mixhead. The change in

potential energy from the inlets to the exit of the mixhead is very small, and is therefore neglected.

$$\sum_{i=1}^{2}(p_i - p_3) + \sum_{i=1}^{2}(\frac{\rho_i V_i^{\,2}}{2} - \frac{\rho_3 V_3^{\,2}}{2}) + \sum_{i=1}^{2}(\rho_i g z_i - \rho_3 g z_3) = \frac{P\ (W)}{Q\ (m^3 s^{-1})} \quad (1)$$

Energy contribution (ΔPE, J/s) from the pressure drop (Δp) due to fluid flow (Q, m^3/s) across the mixing volume is:

$$\Delta PE = \Delta p.2Q \quad (2)$$

Where Δp, pressure drop (N/m^2), was determined by measuring the hydrostatic pressures at the CIJ inlets and exit and taking an average i.e.

$$\Delta p = \sum_{1}^{2}\frac{p_i - p_3}{2} \quad (3)$$

As contribution from turbulent kinetic energy (TKE) is less than 0.25% of the mean value, it is neglected in kinetic energy dissipation calculations. Change in mean kinetic energy was calculated from the inlet and exit flow velocities (V_i, m/s).

$$\Delta KE = \sum_{i=1}^{2}\frac{\rho_i V_i^{\,2}}{2} - \frac{\rho_3 V_3^{\,2}}{2} \quad (4)$$

Energy dissipation rate within the mixing volume is therefore:

$$\varepsilon_{mean} = \frac{\Delta p.2Q + \Delta KE}{\rho V_{mix}} \quad \text{i.e.} \quad \varepsilon_{mean} \propto Q \ \text{ and } \ \varepsilon_{mean} \propto \mathrm{Re}_{jet} \quad (5)$$

Where, ρ and V_{mix} are fluid density (kg/m^3) and mixing chamber volume (m^3) respectively.

3.2 Effect of multiple passes

In the second section, the recirculation effect of the emulsified system through mixheads MH-1 and MH-2 on emulsion drop size and size distributions is analysed. The higher the number of passes, the longer is the residence time of the emulsion inside the mixhead, and therefore, the smaller the drops should become until they reach an equilibrium size. The recirculation allows time for continuous breakup of the drops under constant shear, as well as for surfactant molecules to adsorb over the newly formed drops and thus prevent re-coalescence. The same four surfactant formulations were tested in mixhead MH-1 for up to ten passes under fully turbulent flow conditions (843 mL/min and $Re_{jet} \approx 17{,}900$).

Figure 4 (a) shows that all the emulsions, irrespective of the surfactant formulation, reached their stable equilibrium sizes after six or seven passes. Expectedly, data plots show that the SDS-PGPR formulation delivered the smallest drop size after six passes, followed by the SDS-only system, Tween 20-PGPR, and finally the Tween20-only formulation. Drop sizes for the last two emulsifier/emulsifier formulations were, however, very similar to each other. Of the four formulations, PGPR worked more synergistically with SDS than Tween20 under full turbulence. Drop size data from the first and the sixth passes are compared directly in Table 1, which reconfirm the observations made above. Further, the effect of multiple passes or recirculation on drop size distributions is discussed.

Drop size distributions in Figure 4 (b) for Tween20 stabilized system record a gradual shift with recirculation. The equilibrium for the emulsified system was reached within six to seven passes; any further recirculation had limited effect on mean drop size and size distribution. The shift of the peak from that of the fifth pass to the tenth was not as significant as that from

the first to the fifth. Moreover, looking at the left hand side of the area under the curves, there was a considerable increase in the volume percentage of smaller drop with multipass recirculation. The micrographs (not presented here) confirmed the trends in drop size data obtained from DLS technique.

Figure 5 compares the recirculation results from the MH-1 and MH-2 schemes for fully turbulent flow condition for Tween20 surfactant. Data show a gradual reduction in drop size with recirculation irrespective of the mixhead configuration. Having reached the full turbulence limit at the test flow rates (610 and 843 mL/min, respectively), there was no noticeable reduction in mean drop size after the sixth or seventh pass. Equilibrium drop size data shows that the two geometries fare well in introducing turbulence to the emulsion system but the coalescence mechanism are somewhat different and endup producing differently sized drops. Evidently, back-step reaction step (i.e. coalescence) is significantly more favoured over the breakup step in MH-1 despite having identical Tween20 concentration. Production of larger drops in MH-1 could be attributed to higher collision rates despite operating at a higher Reynolds number (17,900) than MH-2. This data provides some direct evidence of shear induced drop coalescence mechanism.

3.3 Effect of in situ sonication

Aiming for submicron emulsion drop size, we realized that multiple-pass recirculation may not be enough and secondary drop breakup mechanism may need to be promoted. Earlier studies have shown successful integration of *in situ* sonication with other emulsification processes, such as those in homogenizers and in stirred tanks[21]. Based on effective design considerations[25], mixhead MH-2 was modified to accommodate a flat-tipped ultrasonic probe

(3.18 mm diameter) within the hemispherical section of the cylindrical mixing chamber. The resulting geometry was mixhead MH-3 which could help to minimize low velocity regions in the flow field with turbulence emancipating from ultrasonication. In follow on experiments, CIJ operating at full turbulence and maximum flow rate of 610 mL/min (Re_{jet} = 13,000), Tween20 emulsified o/w system was passed through mixhead MH-3 at varying sonication amplitudes of 0% (no sonication), 20%, 30%, and 40% to determine the optimum amplitude value for drop size reduction. Drop data in Figure 6 (inset) clearly shows that smallest drops were obtained at the sonication amplitude of 30% where drop size leveled off, showing little change in drop size with further increase in ultrasonication amplitude. To ensure sufficient turbulence, higher sonication amplitude (40%) was chosen for all subsequent runs. The experiments were repeated at least three times for error estimations.

Considering 40% sonication amplitude as the base case, the recirculation procedure was then implemented with in situ sonication in mixhead MH-3 at full turbulence of 610 mL/min (Re_{jet} = 13,000). At first, 5 vol% sunflower oil containing 1 wt% Tween20 was dispersed in aqueous phase to consider the effect of sonication on emulsion drop size. These results were compared with an emulsion sample subjected to an equivalent number of passes without sonication (0% amplitude) and are presented in Figure 6. The drops obtained with sonication were significantly smaller than those that were obtained in the absence of sonication. The samples were recirculated upto twelve passes under sonication effect and the drop sizes continued to decrease until they reached an equilibrium size at the tenth pass. The optimum number of passes (tenth cycle) with sonication was significantly higher than the minimum number of passes (sixth cycle) that were required to reach size equilibrium in absence of sonication. This was so because sonication provided additional turbulent energy to increase

drop break up, resulting in drops of mean diameter 700 nm, as shown by the dotted line on the plot.

Sonication experiments were repeated using 10% (v/v) of sunflower oil to observe the effect of a higher oil phase volume on the drop size. Surprisingly, similar drop sizes were obtained at both oil concentrations, when supposedly, 10% (v/v) oil should have resulted in larger drops in comparison to 5% oil (v/v) sample. This data indicates that 1 wt% of Tween20 was still sufficient to stabilize the large number of smaller drops that were present in the 10% (v/v) emulsion sample. Supposedly, the shear force in the sonic-jet configuration was large enough to offset the turbulence dampening arising from a higher oil fraction which may have given rise to larger drops.

Tables 2 lists sonic energy dissipation rates (volume averaged mean, ε_{mean}) in mixhead MH-3, obtained at varying amplitudes. At low sonic efficiency (3.9%), sonic dissipation rate was roughly 10^4 W/kg, while at 50% efficiency sonic dissipation was an order of magnitude larger, i.e., 10^5 W/kg. Irrespective of the efficiencies, energy dissipation rate from the probe increased with sonication amplitude. To evaluate the effect of sonication on drop size, the sonic energy added to the system is compared to jet turbulent energy and the data is presented in Table 3. It must be noted that while jet turbulence is a function of feed flow rate, sonic energy varies with sonication amplitude. At 10% amplitude, energy dissipation from the combined mechanisms (jet hydrodynamics and sonication), at all sonic efficiencies, were at least an order of magnitude larger than the energy dissipated from the jet. The same was true at the probe amplitude of 40%. Furthermore, the mean dissipation at 40% amplitude was three times larger than the mean value at 10% amplitude.

Henceforth, we note that at 40% sonication amplitude, sonication energy alone is at least 10 times to 100 times larger than the jet-induced 'mean' energy dissipation (ε_{mean}, volume-average) in the mixhead, and atleast 1 to 3 times larger than the jet-induced 'peak' energy dissipation (ε_{max} at impingement point). Thus, in either case, *in situ* sonication will act in synergy with jet turbulence to further reduce the drop size. The effect of this synergy is presented in Table 4 where with experimental progression, submicron drops (≈ 700 nm mean d_{32}) were obtained at 40% sonic amplitude. We also saw that drop size data obtained after ten passes was equal to the eddy size at full turbulence (Kolmogorov length scale), indicating that emulsification occurred in a turbulent-inertial regime. In addition, the obtained drop sizes were similar to the 'smallest' eddy size, which means that under the combined mechanisms all the drops experienced peak turbulence within the impingement-region of the jets. Table 3 presents shear rates (γ) experienced by drops within the mixhead. These shears are typically several orders of magnitude larger than for the other known mixing devices. Shear rates, γ, are given by expression 6 where ε is the rate of energy dissipation (W/kg) and v_c is the continuous phase kinematic viscosity (m^2/s).

$$\gamma = \left(\frac{\varepsilon}{\upsilon_c} \right)^{1/2} \tag{6}$$

For the purpose of depicting experimental progression so far, Figure 7 is presented. It presents the shift in drop size distribution to the left, favouring production of smaller drops over the course of experiments from the first pass at the best-identified flowrate to the maximum number of cycles at the best-identified flow conditions and finally, to the optimum number of passes at the optimum *in situ* sonication intensity. Ultimately, emulsion drops of sizes around 600 to 800 nm were achieved by integrating *in situ* sonication with sample recirculation in

mixhead MH-3 (Figure 1 c). The drop sizes were in agreement with the DLS data. Furthermore, through Figure 8 (a) it is clear that nearly half of the drops in both 5% (v/v) and 10% (v/v) samples were submicron in scale, where a tiny fraction of them represented nanoemulsion (less than 100 nm diameter). Also, Tween20-PGPR formulation produced comparable drop size as with Tween20 alone. This was only possible when the interface was fully saturated with smaller Tween20 molecules leaving little unpacked regions for the larger PGPR molecules to adsorb.

This lab scale procedure as illustrated in Figure 8 (b) using a single mixhead can be used to produce up to 1.8L/min of emulsion through 24-hour operation and is potentially promising for continuous production of submicron and nanoemulsions at the laboratory scale. Pilot scale up can be achieved by using a series of mixheads in parallel. In the next section, we consider the stability aspects of the produced emulsions.

3.4 Emulsion stability and other considerations

To determine the stability of the emulsions, Tween20 stabilized emulsions produced in MH-3 at 40% sonic amplitude and full turbulence were regularly observed over a period of several weeks under room conditions. The corresponding data is presented in Figure 8 (a). No significant shift in drop size distribution was recorded in 5% and 10% sunflower oil samples over the testing period. No secondary peaks and therefore no evidence of Oswald ripening were recorded over the shelf life of five weeks.

With a target to produce nano drops, limiting drop coalescence at high breakage rates may in drop size. There are a few ways in which this could be achieved, namely by reducing drop collisions post drop breakup, using co-emulsifiers of small molecular size and optimizing

residence time within a mixhead to achieve flash stabilization of the produced drops. Drop breakup may also be enhanced by slightly pressurizing the feed streams to reduce the mixing timescale of the colliding jets, though this may increase drop collision rates as well. The later may partly be achieved by optimizing the dimensions of the exit hose of the mixhead and limiting drop residence time within the mixing zone.

Earlier, the authors[13] have reported variations in mean drop sizes for identical viscosity silicon and sunflower oils with Tween20 emulsifier. Sunflower oil produced smaller drops under identical flow conditions. The variation in drop size could therefore be linked to the oil/emulsifier adsorption chemistry and the adsorption kinetics including the number of active sites at the oil/water interface. Evidently, the hydrophobic forces driving the adsorption of Tween20 molecule on sunflower oil/water interface are stronger than those at the silicone/water interface, which results in lower equilibrium interfacial tension (≈ 6 mN/m) as compared to silicone oil (≈ 9 mN/m). Therefore, oil/surfactant adsorption and physiochemical interactions clearly have great influence on the drop size. These observations are confirmed by drop size distribution obtained for the two oil systems (Figure 9). In the figure, whereas drop size distribution for sunflower oil is more or less unimodal, the one for silicon oil is bimodal. This may be due to unequal adsorption and packing of Tween20 molecules on selective interfaces. Surfactant adsorption on sunflower oil appears to be fast and uniform which may not be the case with silicone oil, resulting in bimodal size distribution. Interfacial tension gradients seem to have developed because of slower Tween20 adsorption on the silicone oil/water interface, causing inhomogeneous breakup of the drops, resulting in multimodal distribution.

As seen earlier, both SDS and Tween20 produced somewhat similar drop sizes with sunflower oil (Figure 2) under fully turbulent conditions. In this case, we can safely argue that final drop size is strongly determined by the drop collision step, provided the interface is fully stabilized. Bigger drops, therefore, form not necessarily due to failure to break up, but due to successful coalescence in the absence of sufficient stabilization. The following section takes a view of some of the intermediate process steps that occur during emulsification to successfully explain the experimental observations.

3.5 Relative effect of mixing and other process timescales

For drops to coalesce they must collide and stay together for a finite time. This makes relative timescales of the associated process steps equally important as the magnitudes of the participating fluid and interparticle forces such as inertial, turbulent, surface, viscous, steric, etc. These timescales include eddy lifetime, drop deformation timescale, film drainage, drop-drop contact, flow fluctuations, micro-mixing timescales, and mixhead residence time which influence the duration of interactions between the drops in a dynamic field causing them to deform, disrupt, and/or coalescence.

Eddy lifetime (τ_{eddy}) in turbulent flow conditions is one of the most well-defined parameter which is defined as the rate of eddy disintegration in a turbulent flow field. When an emulsifier is present in continuous phase, emulsifier adsorption timescale[28], τ_{adsorp} is the sum of convective and diffusive timelengths that the emulsifier molecules take to be transported to the interface prior to formation of physiochemical bonds on the interface. Mixhead residence time (τ_{res}) is the time the drops spend in the mixhead before exiting the mixer and it is expected to be longer than either of the above timescales. Furthermore, in the turbulent

regime, mixing time (τ_{mix}) for mixhead (MH-2) can be estimated by expression 14 whose derivation can be found elsewhere[25]. This mixing time is the micromixing timescale based on Kolmogorov 'turbulence' lengthscale and momentum diffusivity. Mixing time and some other timescales are, therefore, tunable by changing Re_{jet} and fluid properties. These timescales are mathematically expressed as:

$$\tau_{eddy} = \left(\frac{\upsilon_c}{\varepsilon} \right)^{1/2} \qquad (d_p \sim \lambda_k, \text{ Kolmogorov microscale}) \qquad (7)$$

Where v_c is the continuous phase kinematic viscosity (m^2/s), ε is volume average mean or peak or max energy dissipation rate (W/kg), and d_p is mean drop size, d_{32} (m). Whereas ε_{mean} was computed from expression 5, ε_{max} was determined computationally for a wide range of flow conditions[25], some of which are listed in Table 3.

Timescale of turbulence fluctuations in a turbulent flow field is given by:

$$\tau_{fluct} = \left(\frac{{d_p}^2}{\varepsilon} \right)^{1/3} \qquad (d_p > \lambda_k, \text{ Kolmogorov microscale}) \qquad (8)$$

Adsorption timescale of surfactants present in vicinity of o/w interface i.e. a drop dispersed in continuous fluid is given by the following expression[28].

$$\tau_{adsorp} = \frac{\delta_{diff}^2}{D_{ew}} + \frac{h - \delta_{diff}}{u} \qquad (9)$$

Where D_{ew} is surfactant diffusivity (m^2/s), δ_{diff} is the diffusion path length covered by surfactant (m), $h-\delta_{diff}$ is the convection length covered by surfactant and u is the characteristic flow velocity (m/s).

Diffusivity of surfactant molecules and convective length through the continuous phase to the drop interface are given by:

$$D_{ew} = \left(\frac{k_B T}{3\pi \mu_c d} \right) \tag{10}$$

$$h = \left(\frac{{d_p}^2}{16} + \frac{\Gamma d_p}{2C_o} \right)^{1/2} - \frac{d_p}{4} \tag{11}$$

$$\delta_{diff} \sim d_p \, Pe^{-1/2} \tag{12}$$

Where k_B is Boltzmann constant (1.38×10^{-23} $m^2.kg/s^2.K$), T is the temperature (K), μ_c is continuous phase viscosity (kg/m.s), d is surfactant molecule size (m), Γ is the emulsifier moles per unit interface area (mol/m^2), C_o is emulsifier bulk concentration (mol/m^3) and Pe is Peclet Number.

Mixing timescale[25] for confined impinging jet mixhead is given by:

$$\tau_m = K_{CIJR} \frac{\nu_c^{\frac{1}{2}} \Delta^{\frac{3}{2}} d_1^{\frac{1}{2}}}{2V_1^{\frac{3}{2}}} \frac{1}{\left[\left(\frac{\rho_1}{\rho_3} \right)^{\frac{1}{2}} \right]} \frac{1}{\left[\left(1 + \frac{\dot{m}_1}{\dot{m}_2} \right)^{\frac{1}{2}} \right]} \tag{13}$$

or simply, $\tau_{mix} = 1470 \frac{1}{4} \left(\frac{\nu_c}{\varepsilon} \right)^{1/2}$ (14)

Where, Δ, d, V, ρ_i m_i, υ_c and ε are aspect ratio, inlet jet diameter (m), jet velocity (m/s), fluid density (kg/m^3), mass flow rate (kg/s), continuous phase kinematic viscosity (m^2/s) and energy dissipation rate, respectively.

And the timelength spent by the drops undergoing breakup within the mixhead i.e. residence time of mixhead is:

$$\tau_{res} = \frac{V_{mix}}{2Q} \tag{15}$$

Where V_{mix} is the mixing chamber volume (m^3) and Q is the incoming jet flow rate (m^3/s).

An analysis of these timescales illustrates the competing mechanisms in a turbulent flow field generated by the combined jet flow and ultrasonication. We see that on substitution of process parameters with energy dissipation ε_{max}, all intermediate processing steps for Tween20 stabilized system under fully turbulent conditions are completed within the micromixing time of 10^{-4} sec. For all Tween20 stabilized data (best case) in turbulent flow and particularly Figure 7, mixing timescale (10^{-4} sec) is an order of magnitude shorter than drop residence time in the mixer (10^{-3} sec). Furthermore, since the emulsifier adsorption timescale (10^{-8} sec) is two orders of magnitude smaller than turbulence fluctuation timescale (10^{-6} sec) and eddy lifetime (10^{-6} sec), the drops are fully stabilized at all times (i.e. flash stabilized) and are unlikely to coalesce. The timescales obtained for mean energy dissipation (ε_{mean}) corresponding to average flow conditions in mixhead differ by an order of magnitude, but the same relative trends between the above timescales are preserved.

3.6 Performance comparison of CIJ with conventional nano-emulsification techniques

The custom-built CIJ mixer allowed improvement over the design and operational pressures of the conventional microfluidizer and HPH equipment. The major advantage of CIJ is the low operating pressure which can reduce the capital and operational costs of the equipment including maintenance of the production line. CIJ can be manufactured relatively easily, at low dollar cost using simple machining tools. Simple design of CIJ makes it easy to customize the geometry for production of a range of drop sizes. Excessive high pressures[4, 16, 29] (>22,000 psi) have been found to be necessary to produce <200 nm drops, whereas, as shown earlier, ~500 nm drops could be directly fabricated using a simple CIJ mixer under atmospheric conditions. Thus, shear-sensitive/pressure-sensitive products may be saved from over processing unless the intended drop size range is 200 nm and smaller.

Table 5 presents typical drop size distributions obtained in HPH, microfluidizers and CIJ under optimum working conditions. The data indicates that HPH and microfluidizers are capable of delivering drops smaller than 200 nm but only at operating pressures >20,000 psi. On the other hand, CIJ can produce drops as small as 500-700 nm at just about atmospheric pressure, thereby reducing the operational requirements of high pressure equipment.

4.0 CONCLUSIONS

We have reported the working regimes of a simple confined impinging jet mixer which is highly robust in operation and is capable of synthesizing submicron emulsions with throughput of up to 1.2 L/min. This is significant, given the compactness of the design and

easy fabrication; henceforth, it presents an effective platform for development of fine emulsions and powders with well-controlled and reproducible properties for specialized applications in the food and pharmaceutical industry. The following conclusions are made:

- Smallest emulsions were obtained under atmospheric conditions, fully turbulent CIJ mixhead conditions i.e. at $Re_{jet} \geq 13{,}000$ and with small head group surfactants. Surfactant formulations delivered smaller drops than single surfactants.

- Confined Impinging Jets (CIJ) is a significant improvement over the existing High Pressure Homogenizer (HPH) and microfluidizer in terms of the operating conditions. It has been shown that though HPH and microfluidizer schemes are capable of producing < 200 nm mean drop size on multiple passes, but they must operate at high pressure conditions[15], typically >20,000 psi. On the contrary, CIJ can produce <700 nm mean drop size at atmospheric pressure conditions. This is a significant improvement over the existing high pressure technologies for comparable product throughput. Whereas <200 nm drops may be better suited for encapsulating bioactives in specialized o/w pharmaceutical formulations[3], submicron emulsions may be sufficient to achieve the right drop size and texture for beverage and food applications[30-31].

- Longer residence time (multiple pass) may translate into longer duration of shear treatments, which may produce micron-size emulsions.

- Conventional methods (impinging jets and sonic cavitation) are limited by the turbulence level necessary to achieve submicron emulsions on their own. In a classical ultrasonic horn, the cavitation effect working on the drops is limited to a small zone immediately adjacent to the transducer surface, delivering a large variation in shear field

across a large volume of fluid. Likewise, mixing performance (shear field) of impinging jets is severely limited by the back pressure and the feed velocities. But by synergetic integration of the two techniques, the limitations of the previous approaches could be minimized, favouring production of submicron disperse phase drops. It can be therefore safely argued that shear intensity or energy dissipation is the limiting variable during emulsification when drop coalescence has been contained. Energy dissipation could, therefore, be manipulated to enhance emulsification performance of a CIJ mixer and to scale up the process.

- The produced submicron emulsions were highly stable under room conditions and negligible change in size distribution was observed over a 5 week test period.

- Besides drop stabilization, analytical estimates show that an alternate strategy to limit drop coalescence is to tune the drop residence time within the mixer to make it smaller than other timescales. Analytical estimates of the surfactant adsorption timescale indicate that the surfactant adsorption timescale may be approximately 10^{-8} sec for Tween20, while eddy lifetimes may be of the order of 10^{-6} sec. Eddy lifetimes often set the upper limit for the engagement of the dispersed drops in a turbulent flow field. Therefore, if the drops are not quickly stabilized, drop size could scaleup with the mixer residence time. The timescales could be tuned by changing the Reynold number and fluid phase properties.

- Submicron drops could be obtained within a mixing and residence times of 10^{-4} and 10^{-3} secs, which demonstrate the high emulsification efficiency of the confined impinging jet

mixer. This makes the mixhead useful for applications that require flash emulsification including incorporation of actives (nutrients, bioactives) in emulsion-based vehicles.

- High intensity of turbulence obtained within the CIJ mixhead, with or without incorporation of sonic energy, has raised some interesting questions about the balance between surface forces and turbulence, drop breakup, interface stabilization and film drainage rates, which have been partly answered in this work. The performance (mechanisms, mixing rates and timescales etc.) and the benefits of this new emulsification approach with other high shear emulsification methods will be discussed in detail in a separate work.

ACKNOWLEDGEMENTS

The authors gratefully acknowledge the financial support from The Royal Society (UK) through Newton International Fellowship and Newton follow-on support to Dr. Shad Siddiqui. This paper is an extension of the paper/ideas presented at RSC/SCI Colloids - Arrested Gels Conference in Cambridge, England and 13th International Hydrocolloids Conference in Guelph, Canada. The authors declare no conflicting interests.

REFERENCES

(1) Benita, S.; Levy, M. Y. Submicron Emulsions as Colloidal Drug Carriers for Intraveneous Administration: Comprehensive Physicochemical Characterization. *J. Pharm. Sci.*, **1993**, *82(11)*, 1069-79.

(2) Sznitowska, M.; Janicki, S.; Dabrowska, E.; Zurowska-Pryczkowska, K. Submicron Emulsions as Drug Carriers Studies on Destabilization Potential of Various Drugs. *Eur. J. Pharm. Sci*. **2001**, *12(3)*, 175-179.

(3) McClements, D.J.; Rao, J. Food-Grade nanoemulsions Formulations, Fabrication, Properties, Performance, Biological Fate, and Potential Toxicity. *Crit. Rev. Food Sci. Nutr.*, 2011, 51, 285-330.

(4) Qian, C.; McClements, D. Formation of Nanoemulsions Stabilized by Model Food-Grade Emulsifiers Using High Pressure Homogenization: Factors Affecting Particle Size. *Food Hydrocolloids*. **2011**, *25(5)*, 1000-1008.

(5) Wang, S.; Wang, H.; Liang, W.; Huang, Y. An Injectable Hybrid Nanoparticle-in-oil Submicron Emulsion for Improved Delivery of Poorly Soluble Drugs. *Nanoscale Res. Lett.* **2012**, *7(1)*, 219.

(6) Tesch, S.; Schubert, H. Influence of Increasing Viscosity of the Aqueous Phase on the Short-Term Stability of Protein Stabilized Emulsion. *J.Food Eng.* **2002**, *52*, 305-312.

(7) Mason, T. G.; Graves, S. M.; Wilking, J. N.; Lin, M. Y. Extreme Emulsification: Formation and Structure of Nanoemulsion. *Condensed Matter Physics*. **2005**, *9*, 193-199.

(8) Norton, I. T.; Spyropoulos, F.; Cox, P. W. Effect of Emulsifiers and Fat Crystals on Shear Induced Droplet Break-up, Coalescence and Phase Inversion. *Food Hydrocolloids*. **2009**, *23*, 1521-1526.

(9) Solans, C.; Izquierdo, P.; Nolla, J.; Azemar, N.; Garcia-Celma, M. J. Nanoemulsions. *Curr. Opin. Colloid Interface Sci.* **2005**, *10(3-4)*, 102-110.

(10) Nakashima, T.; Shimizu, M.; Kukizaki, M. Membrane Emulsification by Microporous Glass. *Key Eng. Mater.* **1991**, *61/62*, 513-516.

(11) Seekkuarachchi, I. N.; Tanaka, K.; Kumazawa, H. Formation and Characterization of Sub-Micrometer Oil-in-Water (o/w) Emulsions Using High-Energy Emulsification. *Ind. Eng. Chem. Res.* **2006**, *45*, 372-390.

(12) Jafari, S. M.; Assadpoor, E.; He, Y.; Bhandari, B. Re-coalescence of Emulsion Droplets during High-Energy Emulsification. *Food Hydrocolloids*. **2007**, *22*, 1191-1202.

(13) Siddiqui, S. W. The Effect of Oils, Low Molecular Weight Emulsifiers and Hydrodynamics on Oil-in-Water Emulsification in Confined Impinging Jet Mixer. *Colloids Surf A Physicochem Eng. Asp.* **2014**, *443*, 8-18.

(14) Perrier-Cornet, J. M.; Marie, P.; Gervais, P. Comparison of Emulsification Efficiency of Protein-Stabilized Oil-in-Water Emulsions Using Jet, High Pressure and Colloid Mill Homogenization. *J. Food Eng.* **2005,** *66*, 211-217.

(15) Lee, L.; Norton, I. Comparing Droplet Breakup for a High-Pressure Valve Homogeniser and a Microfluidizer for the Potential Production of Food-grade Nanoemulsions. *J. Food Eng.* **2013**, 114(2): 158-163.

(16) Lee, L.; Hancocks, R.; Noble, I.; Norton, I.; Production of Water-in-Oil Nanoemulsions Using High-Pressure Homogenisation: A Study on Droplet Break-up. 2014, *J. Food Eng.* 2014, 131: 33-37.

(17) Microfluidics USA, 2017, Pilot Scale and Production Scale Equipment, *https://www.microfluidicscorp.com/microfluidizers/pilot-and-production*

(18) Siddiqui, S. W.; Norton, I. T. Oil-in-Water Emulsification Using Confined Impinging Jets. *J. Colloid. Interface Sci.* **2012**, *377*, 213-221.

(19) Sawarkar, A. N.; Pandit, A. B.; Samant, S. D.; Joshi, J. B. Use of Ultrasound in Petroleum Residue Upgradation. Can. J. Chem. Eng. **2009**, *87*, 329-342.

(20) O'Sullivan, J.; Beevers, J.; Park, M.; Greenwood, R.; Norton, I. Comparative Assessment of the Effect of Ultrasound Treatment on Protein Functionality Pre- and Post-emulsification. *Colloids Surf A Physicochem Eng. Asp.* **2015**, *484*, 89-98.

(21) Monnier, H.; Wilhelm, A. M.; Delmas, H. The Influence of Ultrasound on Micromixing in a Semi-Batch Reactor. *Chem. Eng. Sci.* **1999**, *54*, 2953-2961.

(22) Banert, T.; Brenner, G.; Peuker, U. A. Operating Parameters of a Continuous Sono-Chemical Precipitation Reactor. *Proc. AlChE Meeting, USA*. **2006**, Paper ID 35202.

(23) Graves, S.; Meleson, K.; Wilking, J.; Lin, M. Y.; Mason, T. G. Structure of Concentrated Nanoemulsions. *J. Chem. Phys.* **2005**, *122*, 134703.

(24) Siddiqui, S. W.; Unwin, P. J.; Xu, Z.; Kresta, S. M. The Effect of Stabilizer Addition and Sonication on Nanoparticle Agglomeration in a Confined Impinging Jet Reactor. *Colloids Surf A Physicochem Eng. Asp.* **2009**, *350*, 38-50.

(25) Siddiqui, S. W.; Zhao, Y.; Kukukova, A.; Kresta, S. M. Characteristics of a Confined Impinging Jet Reactor: Energy Dissipation, Homogeneous and Heterogeneous Reaction Products, and Effect of Unequal Flow. *Ind. Eng. Chem. Res.* **2009**, *48*, 7945-7958.

(26) Apenten, R. K. O.; Zhu, Q. H. Interfacial Parameters for Selected Spans and Tweens at the Hydrocarbon-Water Interface. *Food Hydrocolloids*. **1996**, *10*, 27-30.

(27) Kong, L.; Beattie, J. K.; Hunter, R. J. Electroacoustic Estimates of Non-Ionic Surfactant Layer Thickness on Emulsion Drops. *Phys. Chem. Chem. Phys.* **2001**, *3*, 87-93.

(28) Aldana, G. A. P. Effect of Surfactants on Drop Size Distribution in a Batch, Rotor-Stator Mixer. *Ph.D. Thesis University of Maryland, USA*. **2005**.

(29) Donsi F.; Annunziata M.; Sessa M.; Ferrari G. Nanoencapsulation of Essential Oils to Enhance their Antimicrobial Activity in Foods. *LWT – Food Sci. Technol*. 2011, 44(9), 1908–1914.

(30) Henry, J.V.L.; Fryer, P.J.; Frith, W.J.; Norton, I.T. The Influence of Phospholipids and Food Proteins on the Size and Stability of Model Sub-micron Emulsions. *Food Hydrocolloids*, 2010, 24(1), 66–71.

(31) Klein, M.; Aserin, A.; Svitov, I.; Garti, N. Enhanced Stabilization of Cloudy Emulsions with Gum Arabic and Whey Protein Isolate. *Colloids Surf. B*, 2010, 77(1), 75–81.

(32) Yuan Y.; Gao Y.; Zhao J.; Mao L. Characterization and Stability Evaluation of β-Carotene Nanoemulsions Prepared by High Pressure Homogenization Under Various Emulsifying Conditions. *Food Res. Int.* 2008, 41, 61–8.

(33) Wooster, T.; Golding, M.; Sanguansri, P.; Impact of Oil Type on Nanoemulsion Formation and Oswald Ripening Stability, *Langmuir*, 2008, 24(22): 12758-12765.

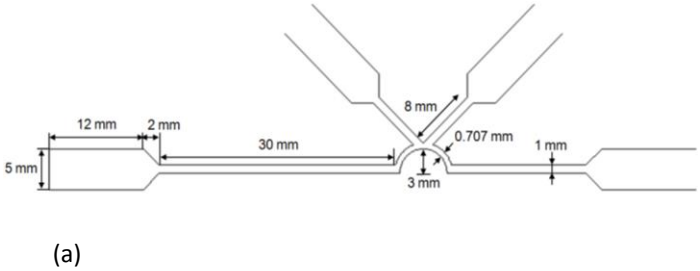

(a)

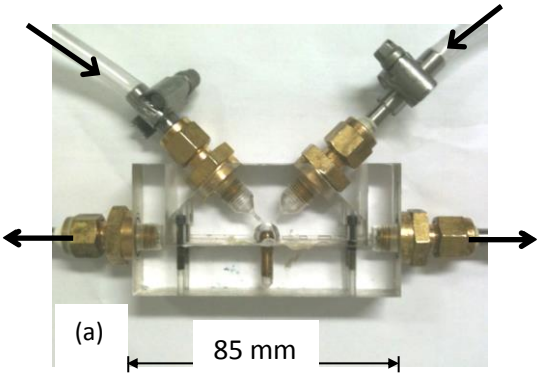

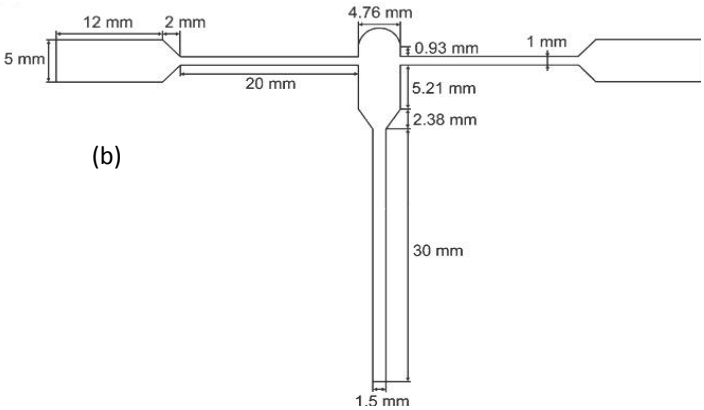

(b)

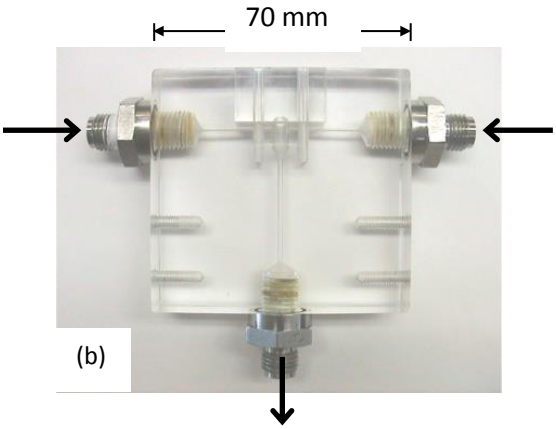

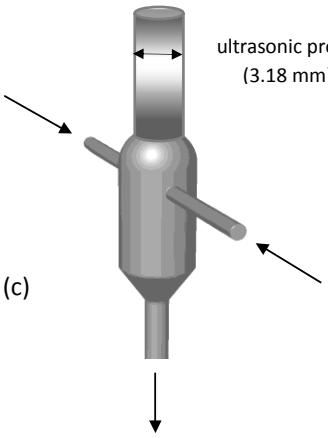

Figure 1: Dimensions of the fabricated mixer schemes (a) MH-1, (b) MH-2[18] and (c) MH-3[24].

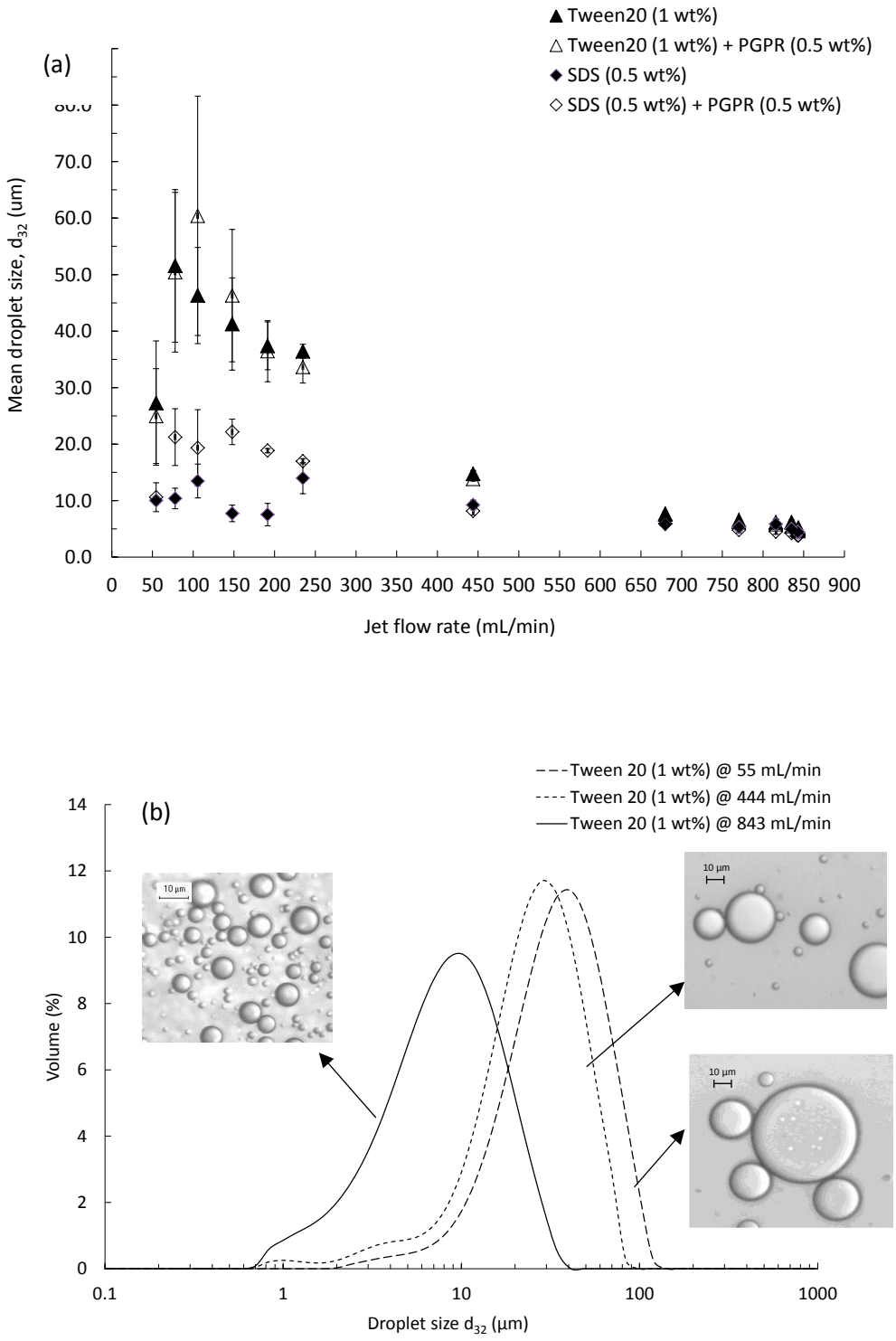

Figure 2: Effect of varying feed flow rate on emulsion (a) drop size and (b) size distribution from mixhead MH-1. Sunflower oil concentration was 5% (v/v).

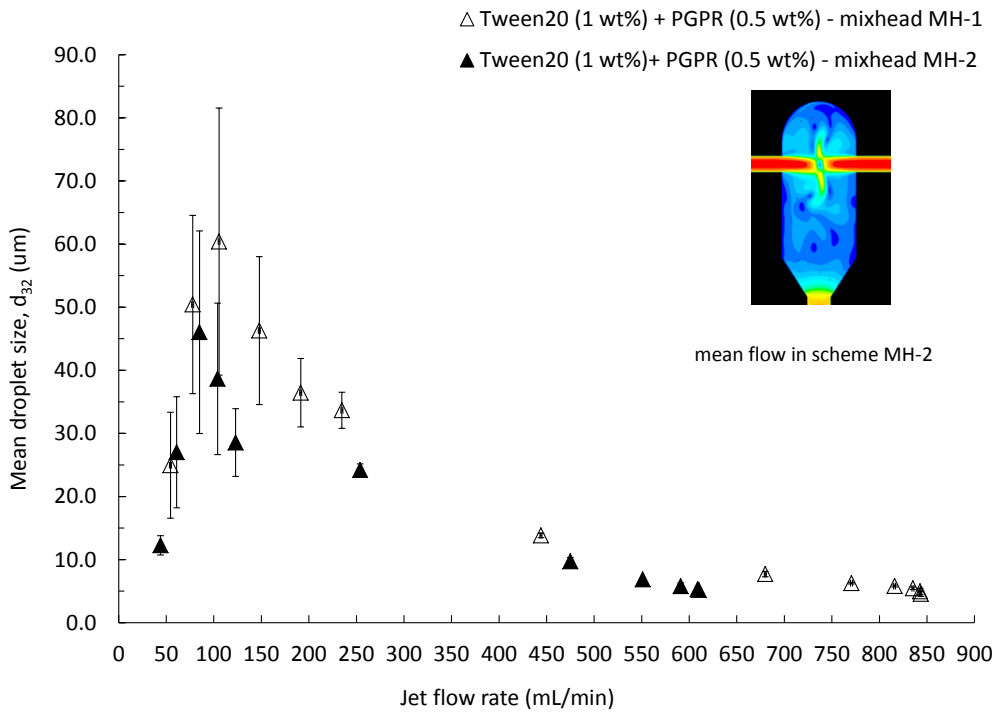

Figure 3: Drop size variation with feed flow rates in mixheads MH-1 and MH-2 in the presence of combined Tween20/PGPR. Sunflower oil concentration was 5% (v/v) while Tween20 concentration was 1 wt% and PGPR was 0.5 wt%. Inset image[25] presents simulated flow field inside a CIJ.

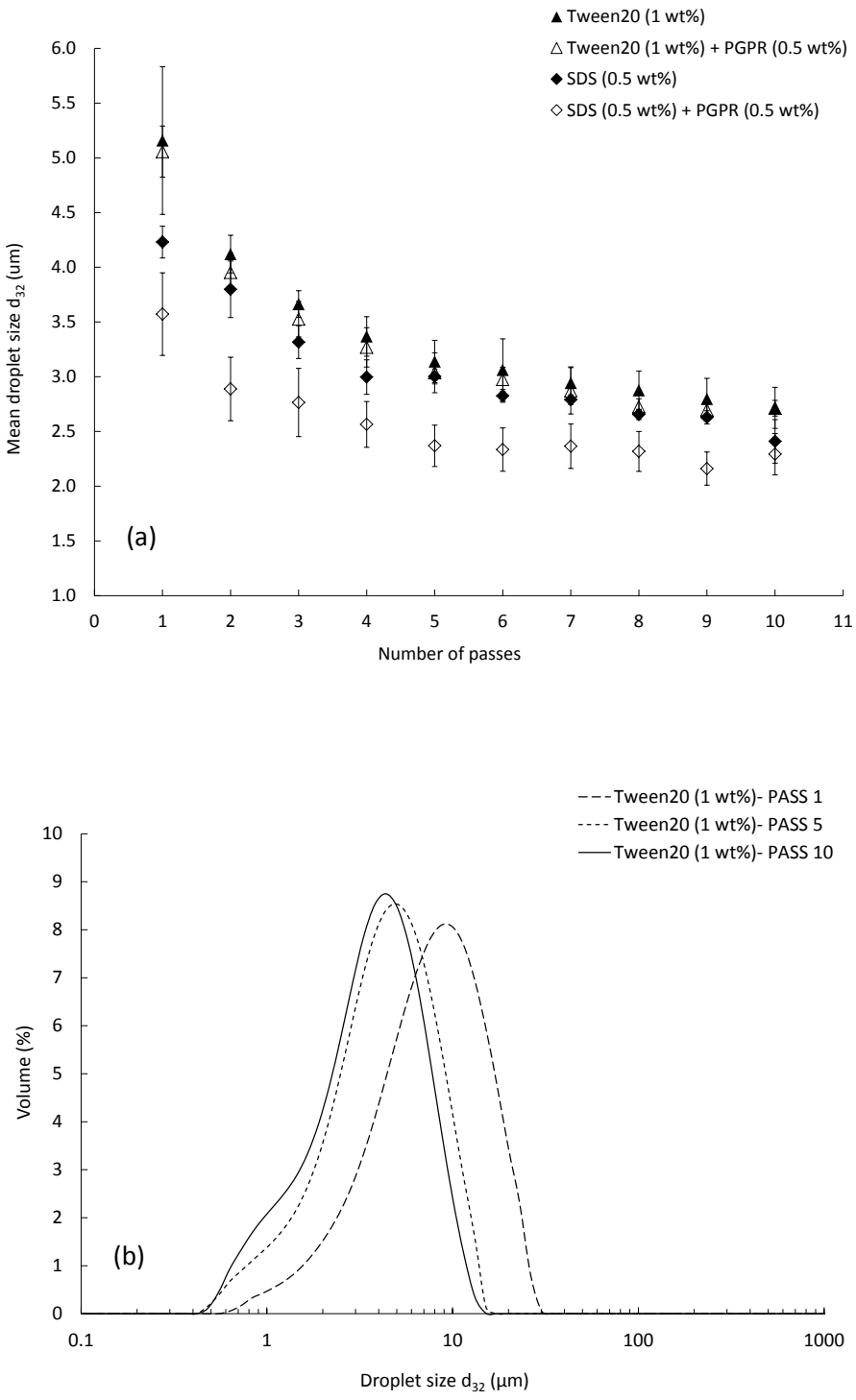

Figure 4: Effect of multiple pass recirculation on emulsion (a) drop size and (b) size distribution in mixhead MH-1 at 843 mL/min ($Re_{jet} \approx 17{,}900$). Sunflower oil concentration was 5% (v/v).

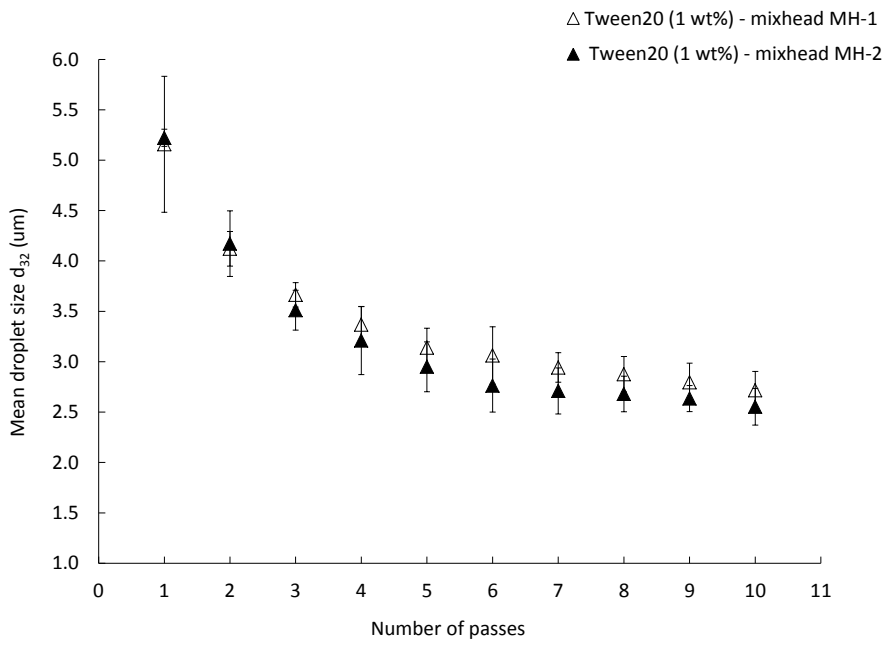

Figure 5: Effect of recirculation on emulsion drop size for mixheads MH-1 and MH-2 at fully turbulent flow of 843 mL/min ($Re_{jet} \approx 17{,}900$) and 610 mL/min ($Re_{jet} \approx 13{,}000$) respectively. Sunflower oil concentration was 5% (v/v).

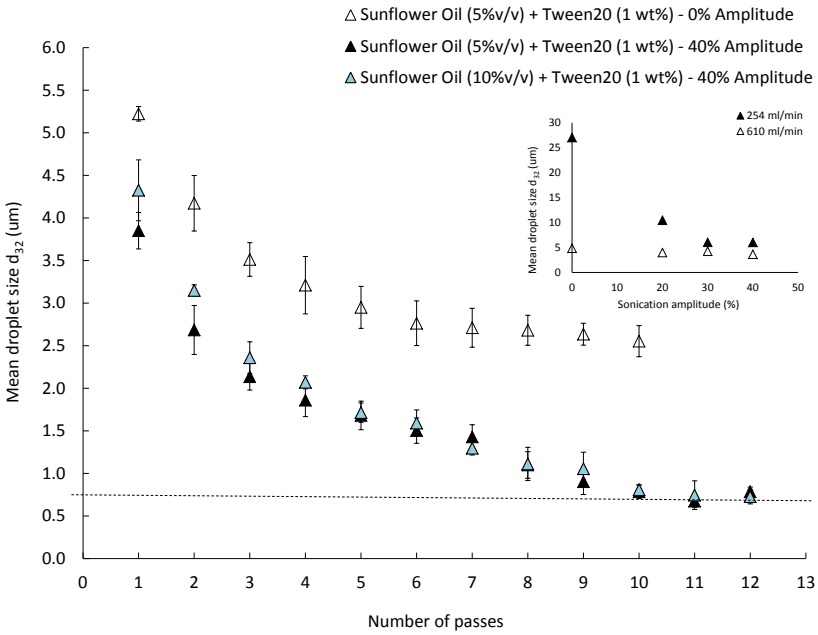

Figure 6: Effect of *in situ* sonication and oil content on multipass recirculation in mixhead MH-3 at full turbulence (feed flow rate = 610 mL/min and $Re_{jet} \approx 13{,}000$). Inset image shows effect of in situ sonication at low and high jet flow rates at oil concentration of 5% (v/v).

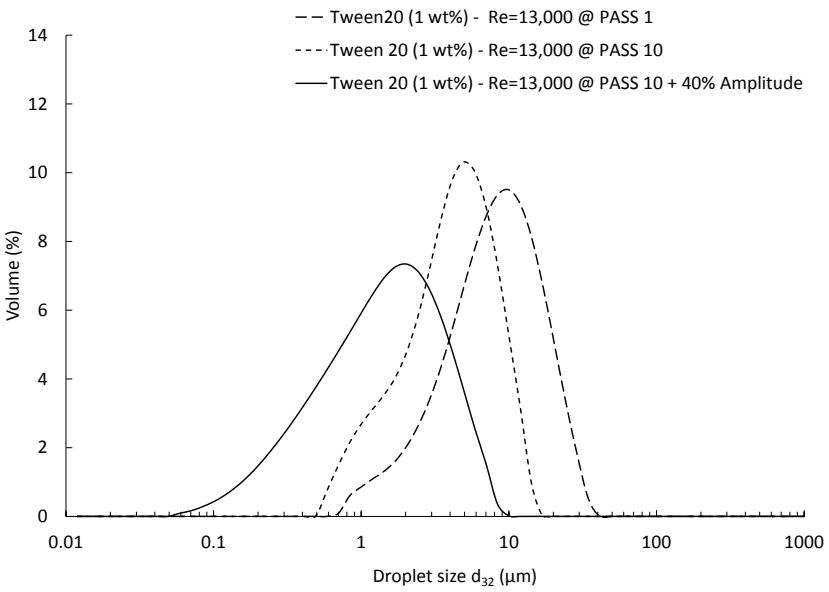

Figure 7: Experimental progress from single pass at full turbulence to tenth pass at full turbulence, to *in situ* sonication synergizing jet-induced turbulence at tenth pass. Concentration of sunflower oil was 5% (v/v).

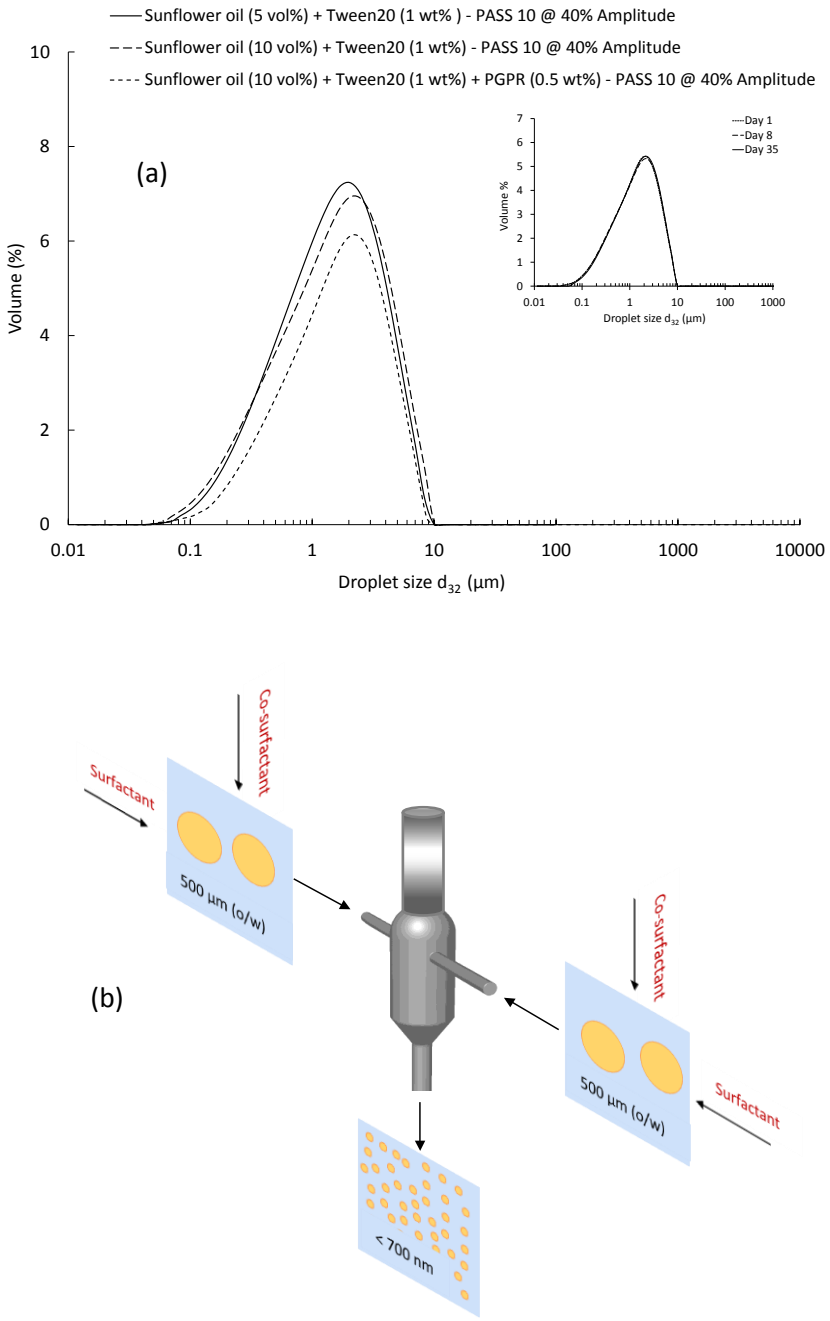

Figure 8: (a) Effect of oil content and emulsifier combination on drop size distribution subjected to in situ sonication and full jet-induced turbulence (feed flow rate = 610 mL/min, $Re_{jet} \approx 13{,}000$). Inset shows emulsion stability at 10% (v/v) oil over 5 weeks. (b) Schematic illustration of the MH-3mixer fitted with an *in situ* sonicator for continuous synthesis of submicron emulsions.

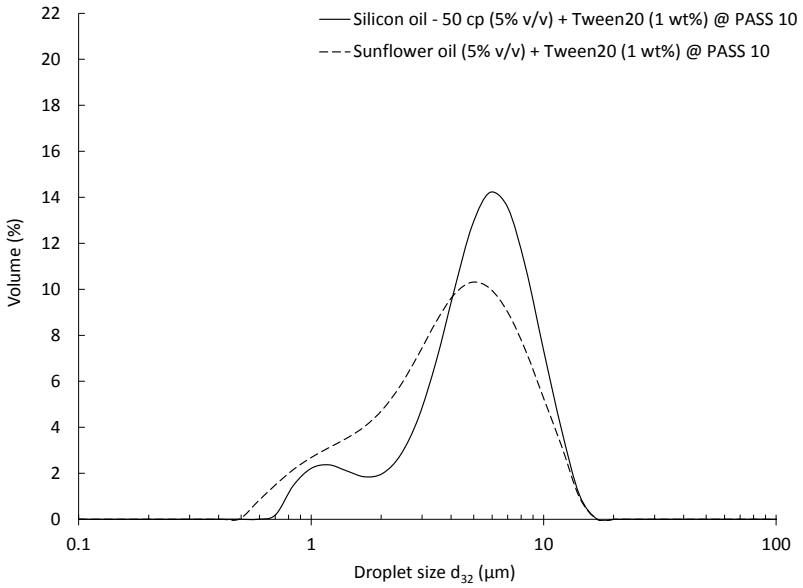

Figure 9: Effect of oil type (organic versus inorganic) on particle size distributions under fully turbulent flow and identical emulsifier conditions. Figure[13] reproduced with modifications to explain a phenomenon.

Table 1: Equilibrium drop size under full turbulence at feed flow rate of 843 mL/min ($Re_{jet} \approx$ 17,900) and multiple passes in mixhead MH-1. Sunflower oil concentration was 5% (v/v).

Surfactant combination (wt%)	**Mean drop size d_{32} (μm)**	
	First pass	Sixth pass
Tween20 (1 wt%)	5.19 ± 0.20	3.06 ± 0.28
Tween20 (1 wt%) + PGPR (0.5 wt%)	4.59 ± 0.43	2.98 ± 0.11
SDS (0.5 wt%)	4.37 ± 0.42	2.83 ± 0.06
SDS (0.5 wt%) + PGPR (0.5 wt%)	3.83 ± 0.36	2.34 ± 0.20

Table 2: Effect of sonic probe amplitude on sonic energy dissipation within mixhead MH-3.

Probe Amplitude (%)	Power input (W)	Sonic energy dissipation, ε_{mean} (W/kg) (at energy conversion efficiency: 3.9% - 50%)[19, 21, 25]
0	0	0
10	50	1.2×10^4 - 1.6×10^5
20	100	2.5×10^4 - 3.2×10^5
30	150	3.7×10^4 - 4.7×10^5
40	200	4.9×10^4 - 6.3×10^5

Table 3: Turbulent energy dissipation (ε) in mixhead scheme MH-3 at assumed ultrasonic conversion efficiencies. Values corresponding to 50% efficiency are in brackets ( ).

	ε (W/kg)	ε_{mean} (W/kg)			ε_{max} (W/kg)		
Sonic probe amplitude (%)	ultrasonics (at 3.9% or 50% energy conv. eff.)	Jet[18] (at 610 ml/min) (W/kg)	Jet[18]+ultrasonics (at 610 mL/min and 3.9% or 50%) (W/kg)	$\gamma_{jet+sonics}$ (s^{-1})	Jet[18] (at 610 ml/min)	Jet[18]+ultrasonics (at 610 mL/min and 3.9% or 50%)	$\gamma_{jet+sonics}$ (s^{-1})
10	$1.2x10^4$ ($1.6x10^5$)	$9.85x10^3$	$2.2x10^4$ ($1.7x10^5$)	$1.5x10^5$ ($4.1x10^5$)	$3.58x10^5$	$3.7x10^5$ ($5.2x10^5$)	$6x10^5$ ($7.2x10^5$)
40	$4.9x10^4$ ($6.3x10^5$)	$9.85x10^3$	$5.9x10^4$ ($6.4x10^5$)	$2.4x10^5$ ($8x10^5$)	$3.58x10^5$	$4.1x10^5$ ($9.9x10^5$)	$6.4x10^5$ ($9.9x10^5$)

Table 4: Turbulence scale and the obtained drop sizes at various process conditions.

Jet flow rate (ml/min)	Kolmogorov eddy size[18] (μm)		Mean drop size, d_{32} (μm)				
	smallest	mean	First pass	First pass	First pass	Tenth pass	Tenth pass + in situ sonication (40% amplitude)
			Tween20 (1 wt%)	SDS (0.5 wt%)	Tween20 (1 wt%) + PGPR (0.5 wt%)	Tween20 (1 wt%)	Tween20 (1 wt%)
254	2.2	6.0	23.2±3.6	8.9±1.1	24.2±0.96	-	-
475	1.5	3.6	9.0±0.3	6.3±0.1	9.7±0.59	-	-
551	1.4	3.4	6.7±0.1	5.4±0.3	6.9±0.13	-	-
610	1.3	3.2	4.6±0.5	3.8±0.07	5.2±0.24	2.5±0.18	0.78±0.09

Table 5: Drop size comparison between high pressure homogenizer, microfluidizer and confined impinging jets.

Oil Phase	**Surfactant**	**Particle size (equilibrium)**	**Technology**	**Reference**
MCT	Tween20, 40, 60, 80	132-148 nm	High Pressure Homogenizer	Yuan et al., 2008
Palm oil, sunflower oil	Soy lecithin, Tween 20	130-236 nm	High Pressure Homogenizer (45,000 psi)	Donsi et al., 2011
Corn Oil, octadecane	Tween 20, sodium dodecylsulfate, beta-lactoglobulin	60-150 nm	Microfluidizer (22,000 psi)	Qian and McClements, 2010
Peanut oil	Tween 80, sodium dodecylsulfate	120 nm	Microfluidizer	Wooster et al., 2008
Sunflower oil	PGPR	112-167 nm	High Pressure Homogenizer, Microfluidizer (22,000 psi)	Lee et al., 2014
Sunflower oil	Tween20, sodium dodecylsulfate	2-4 µm	Confined Impinging Jets	Siddiqui, 2012
Sunflower oil	Tween20, sodium dodecylsulfate PGPR	100 nm to 1 micron	Confined Impinging Jets	Present work

PGPR = Polyglycerol polyricinoleate